Multi-scale representation of deformation via Beltrami coefficients

Ronald Lui

The Chinese University of Hong Kong

香港中文大學
THE CHINESE UNIVERSITY OF HONG KONG

Outline:

- Motivation
- Beltrami coefficient & bijective deformation
- Proposed methods
  - Extraction of bijective deformation
  - Multiscale decomposition of deformations
- Experimental results

Outline:

- Motivation
- Beltrami coefficient & bijective deformation
- Proposed methods
  - Extraction of bijective deformation
  - Multiscale decomposition of deformations
- Experimental results

Motivation

Analyzing shape deformation and extracting the deformation pattern of shapes over time…

Medical imaging: quantify morphology, cardiac motion,…

Graphics: simulation of object motion, animation …

Visions: shape analysis, classification, recognition, video tracking…

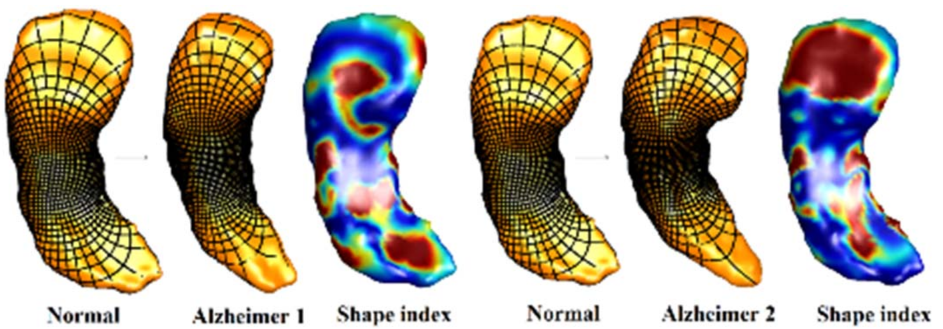

Quantify morphology

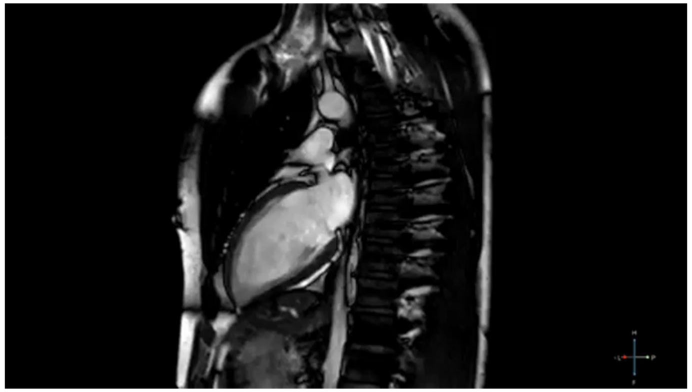

Analysis of cardiac motion

Analysis of deformations

- Shape deformation as a transformation of the domain in which the object is embedded;
- Deformation = Combination of local and global deformations of different scales and locations;
- Focus on: Foldover-free shape deformation (bijective transformation);
- GOAL: Develop an algorithm to decompose a deformation into different components of different scales and locations.

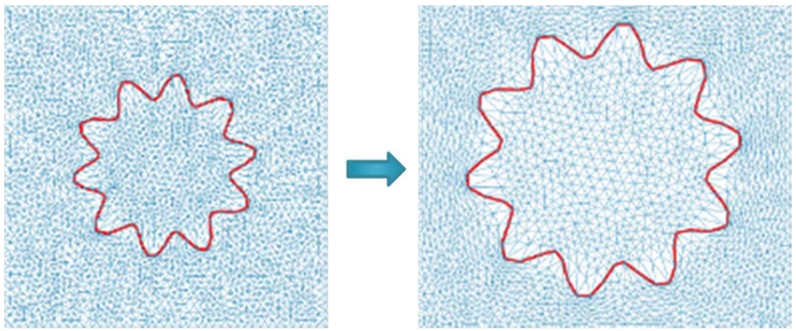

Challenge:

- Each component of the decomposition remains bijective (describe foldover-free deformations at multiple scales);
- Applying multiscale decomposition (e.g. Fourier) on the coordinate functions cannot preserve bijectivity.

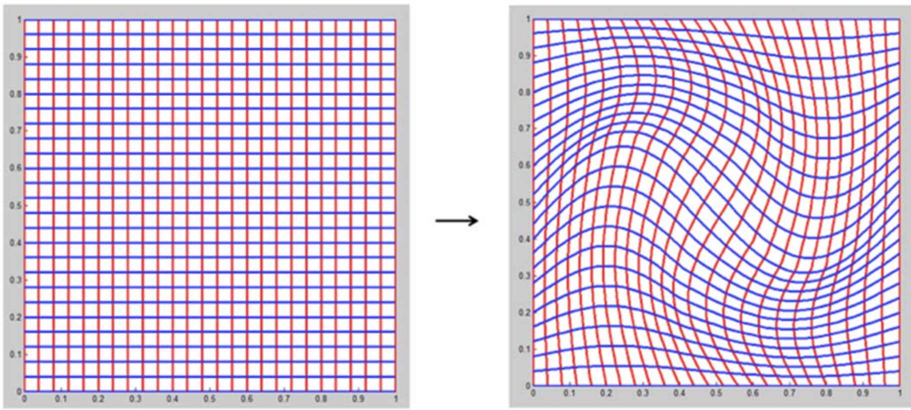

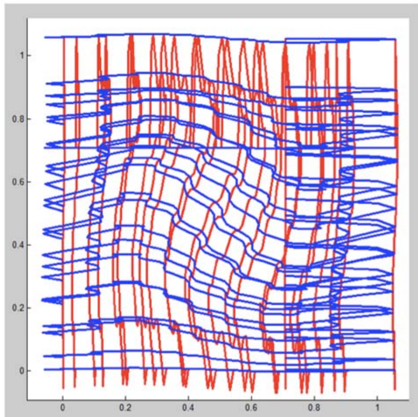

Fourier compression on the coordinate functions

Related works:

- Abeyratne et al.: *apply Cauchy-Navier equation to describe the elastic deformation, a wavelet-based approach is developed for multiscale deformation analysis;*
- Sommer et al.: *proposed multiscale decomposition using multiscale kernel bundle to represent large deformations, under the Large Deformation Diffeomorphic Metric Mapping (LDDMM) framework.*
- Donoho et al. : *proposed morphlet transform to transform a deformation into multiple scales; inverse transform is a bijection;*
- Tong et al.: *proposed variational multiscale decomposition of vector fields*

Propose method:

- Apply the Beltrami coefficient to represent the bijective deformation;
- *Wavelet transform on the Beltrami coefficient to obtain a multi-scale decomposition of a deformation.*

Outline:

- Motivation
- Beltrami coefficient & bijective deformation
- Proposed methods
  - Extraction of bijective deformation
  - Multiscale decomposition of deformations
- Experimental results

Beltrami coefficient & Bijective deformations

- Every orientation-preserving homeomorphism between Riemann surfaces satisfies the Beltrami's equation:

$$\frac{\partial f}{\partial \bar{z}}(z) = \mu(z)\frac{\partial f}{\partial z}(z)$$

  with: $||\mu||_\infty < 1$

- $\mu : S \to \mathbb{C}$ is called the Beltrami coefficient;
- A complex-valued function measuring the local geometric distortion
- Locally, we have

$$\begin{aligned} f(z) &\approx f(p) + f_z(p)z + f_{\bar{z}}(p)\bar{z} \\ &= f(p) + f_z(p)(z + \mu(p)\bar{z}). \end{aligned}$$

Scaling

Stretch map

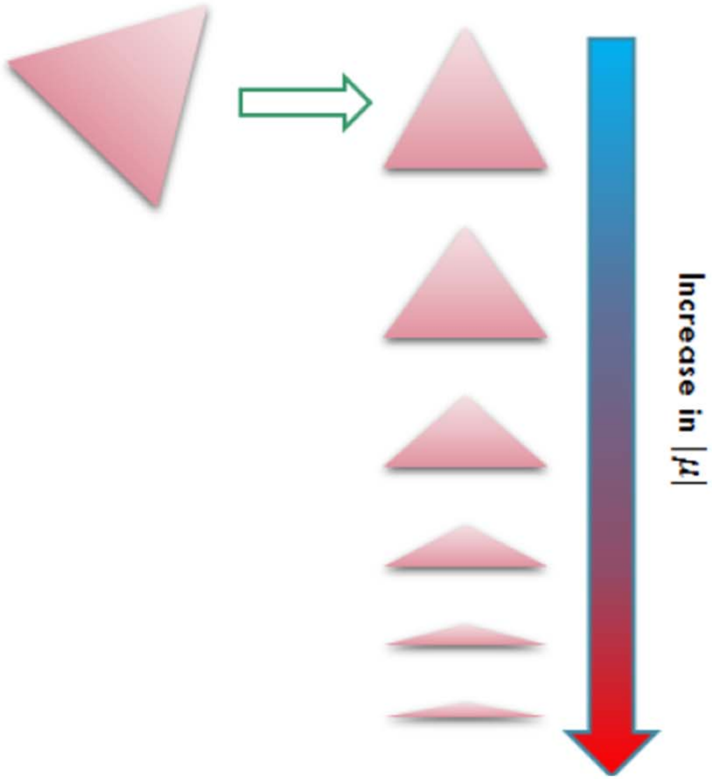

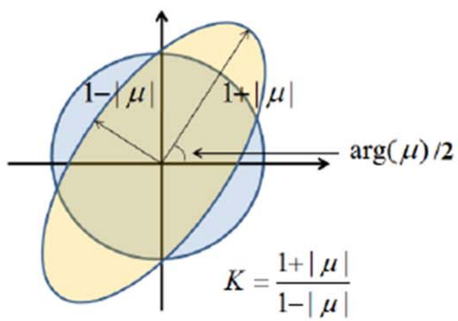

Illustration of local geometric distortion

Example

Original face

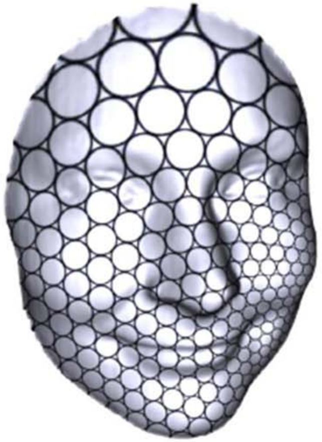

Circle packing

Conformal map
(Circles to circles)

Zero Beltrami coefficient

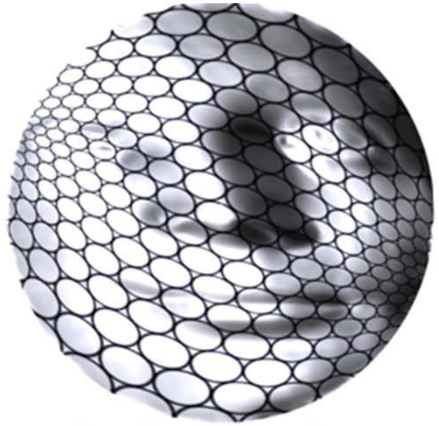

Quasiconformal map
(Circles to ellipses)

Non-zero Beltrami coefficient

Zero BC
(Conformal)

$$f^*(ds_E^2) = \lambda|dz|^2$$

Non-zero BC
(Quasiconformal)

$$f^*(ds_E^2) = |\frac{\partial f}{\partial z}|^2|dz + \mu(z)d\overline{z}|^2$$

Measurable Riemann mapping Theorem

Measurable Riemann Mapping Theorem

Suppose $\mu : \mathbb{C} \to \mathbb{C}$ is Lebesgue measurable satisfying $||\mu||_\infty < 1$, then there is a quasi-conformal homeomorphism ϕ from $\mathbb{C}$ onto itself, which is in the Sobolev space $W^{1,2}(\mathbb{C})$ and satisfies the Beltrami equation. Furthermore, by fixing 0, 1 and ∞, the associated quasi-conformal homeomorphism ϕ is uniquely determined.

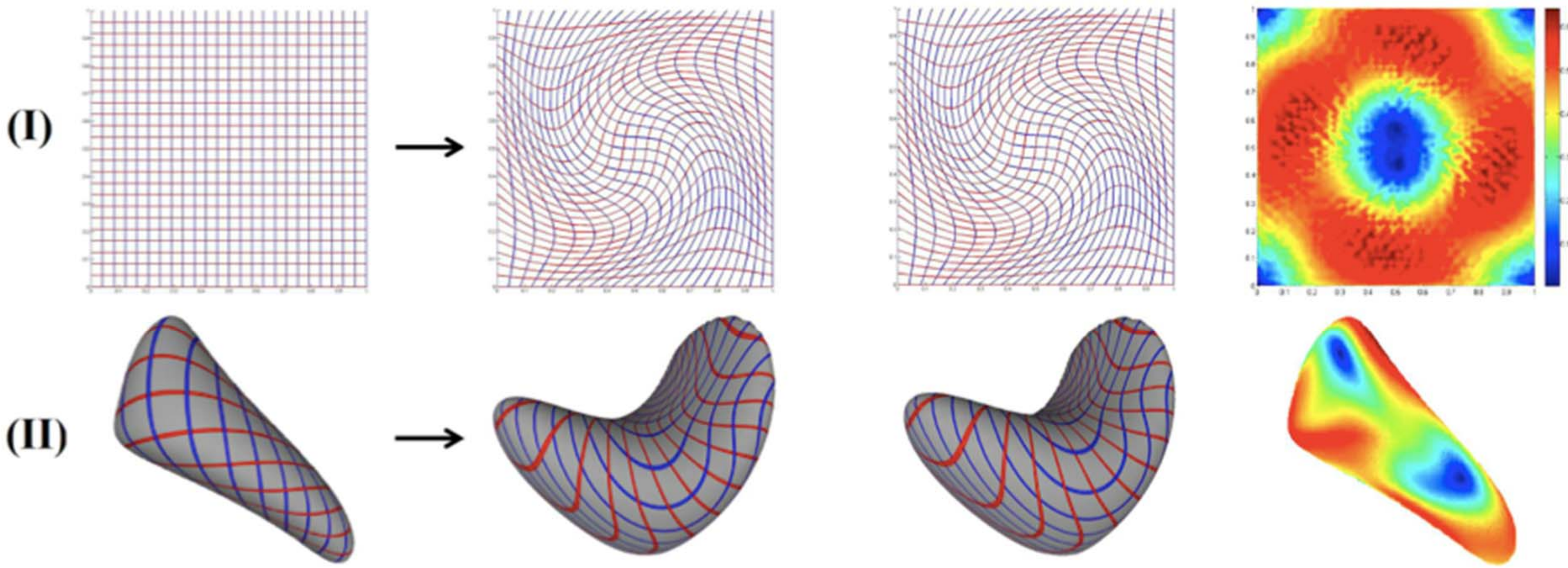

Original diffeomorphism
(A)
Reconstructed diffeomorphism from Beltrami representation
(B)
Beltrami representation
(C)

Reconstruction of deformation from BC

1. Beltrami Holomorphic flow (BHF) method:

[Iterative modification of the mapping according to the variation of BC]

$$
\begin{tikzcd}
\mu_0 = 0 \arrow[r] \arrow[d] & \mu_1 = \mu/N \arrow[r] \arrow[d] & \cdots\ \cdots \arrow[r] & \mu_N = \mu \arrow[d] \\
f^0 = \mathbf{id} \arrow[r, "\mathbf{BHF}"] & f^{\mu/N} \arrow[r, "\mathbf{BHF}"] & \cdots\ \cdots \arrow[r, "\mathbf{BHF}"] & f^{\mu}
\end{tikzcd}
$$

If: $\mu(t)(z) = \mu(z) + t\nu(z) + t\epsilon(t)(z)$

Then: $f^{\mu(t)}(w) = f^{\mu}(w) + t\dot{f}^{\mu}[\nu](w) + o(|t|)$

$$\text{where } \dot{f}[\nu](w) = -\frac{f^{\mu}(w)(f^{\mu}(w)-1)}{\pi}\int_{\mathbb{C}} \frac{\nu(z)((f^{\mu})_z(z))^2}{f^{\mu}(z)(f^{\mu}(z)-1)(f^{\mu}(z)-f^{\mu}(w))}\,dx\,dy.$$

The variation can be approximated by solving the Least Square Beltrami

$$\mathbf{LBS}(\mu) = \mathbf{argmin}_{f\in\mathcal{A}}\{\int_{S_1} |\frac{\partial f}{\partial \bar{z}} - \mu\frac{\partial f}{\partial z}|^2 dS_1\}$$

Experimental results

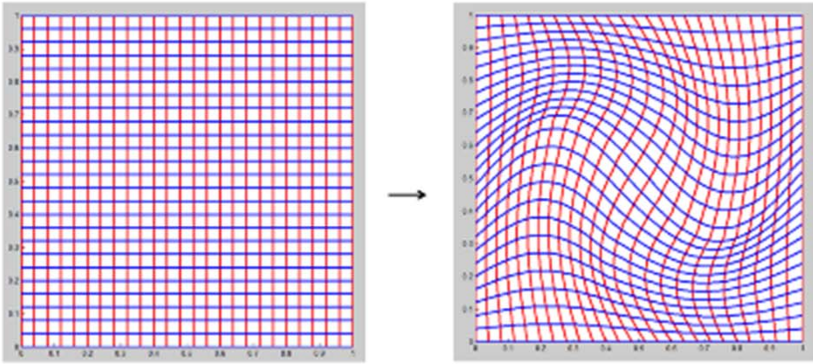

(A)

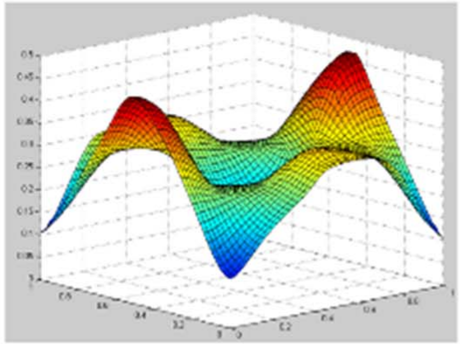

(B)

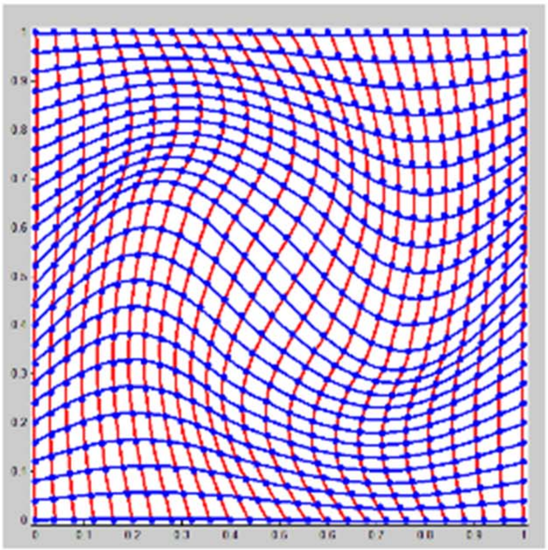

(C)

Iteration	*Error*	*Iteration*	*Error*
1	*0.2674*	*11*	*0.1395*
2	*0.2553*	*12*	*0.1256*
3	*0.2431*	*13*	*0.1114*
4	*0.2307*	*14*	*0.0970*
5	*0.2182*	*15*	*0.0823*
6	*0.2056*	*16*	*0.0673*
7	*0.1927*	*17*	*0.0520*
8	*0.1797*	*18*	*0.0366*
9	*0.1665*	*19*	*0.0210*
10	*0.1531*	*20*	*0.0166*

(D)

Computational algorithms for QC

Linear Beltrami Solver (LBS)

[Converting the Beltrami's equation into elliptic PDEs]

$$\frac{\partial f}{\partial \bar{z}} = \mu(z)\frac{\partial f}{\partial z} \quad \text{(Beltrami's equation)}$$

$$\Downarrow$$

$$\begin{aligned} -v_y &= \alpha_1 u_x + \alpha_2 u_y; \\ v_x &= \alpha_2 u_x + \alpha_3 u_y. \end{aligned}$$

$$\text{where } \alpha_1 = \frac{(\rho-1)^2+\tau^2}{1-\rho^2-\tau^2};\ \alpha_2 = -\frac{2\tau}{1-\rho^2-\tau^2};\ \alpha_3 = \frac{1+2\rho+\rho^2+\tau^2}{1-\rho^2-\tau^2}.$$

Taking divergence on both sides, we get the generalized Laplace's equation

$$\nabla \cdot \left(A\begin{pmatrix} u_x \\ u_y \end{pmatrix}\right) = 0 \quad \text{and} \quad \nabla \cdot \left(A\begin{pmatrix} v_x \\ v_y \end{pmatrix}\right) = 0 \quad \text{where } A = \begin{pmatrix} \alpha_1 & \alpha_2 \\ \alpha_2 & \alpha_3 \end{pmatrix}.$$

Subject to suitable boundary conditions, the above equation can be solved by efficiently conjugate gradient method.

Experimental results

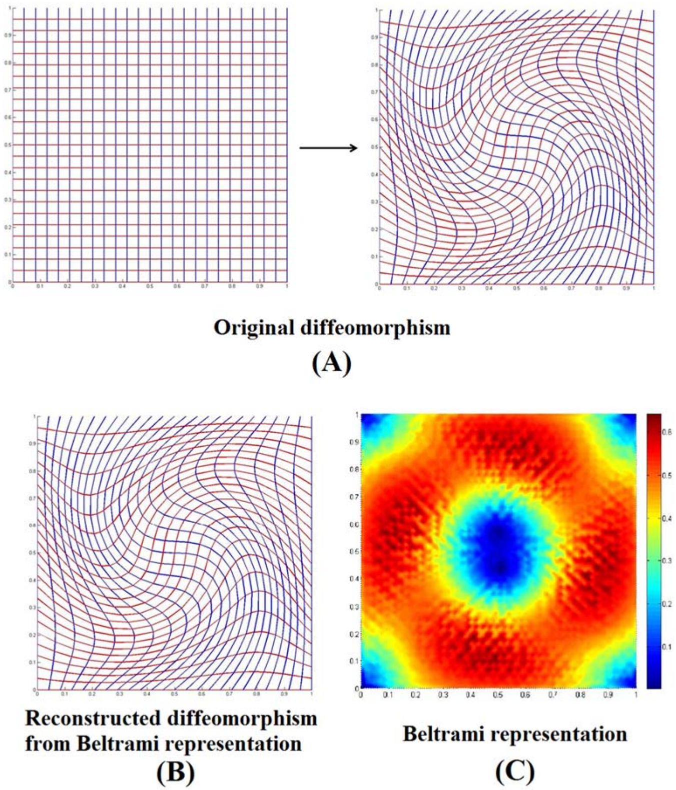

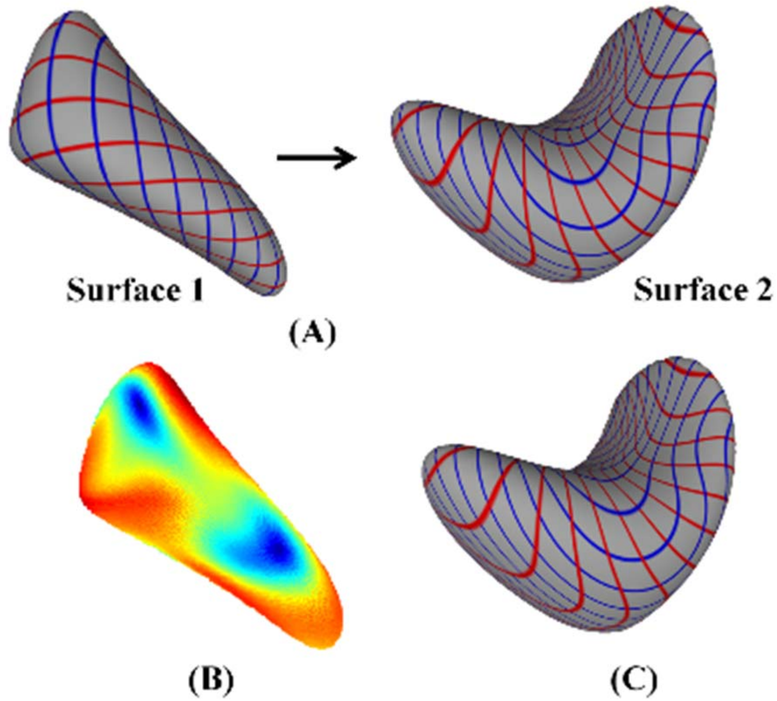

Bijectivity preservation

- *Adjusting the mapping by adjusting the BC can preserve the bijectivity much easier;*
- *Manipulating the mapping through adjusting the coordinate functions may cause flips or folds.*

Demonstration:

Method:
1.Represent bijective surface maps by BCs;
2.Write BCs as Fourier decomposition;

$$\mu(x,y) = \sum_{j,k=-N}^{N} c_{j,k} e^{\sqrt{-1}\pi jx/T} e^{\sqrt{-1}\pi ky/T}$$

3.Truncate the high-frequency components for compression.

Bijectivity preservation

Demonstration:

Fourier decomposition of BC:

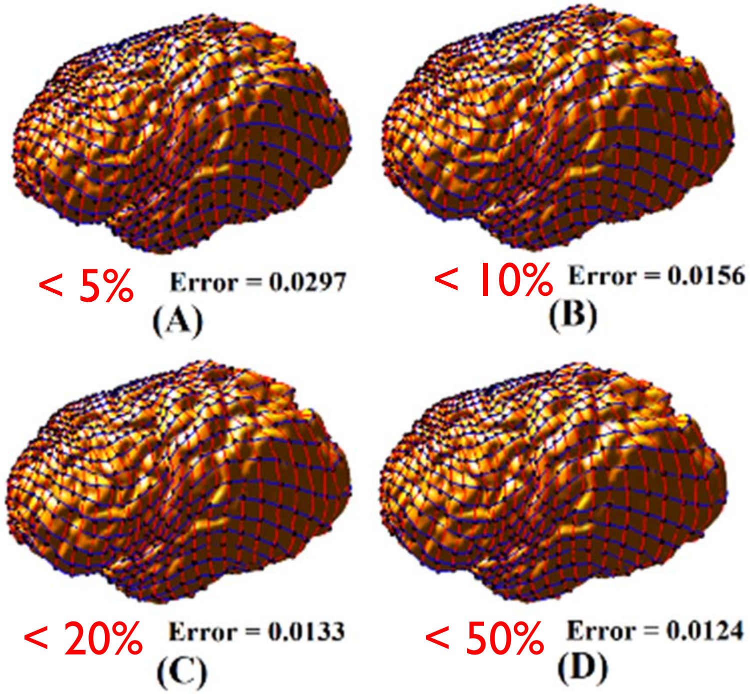

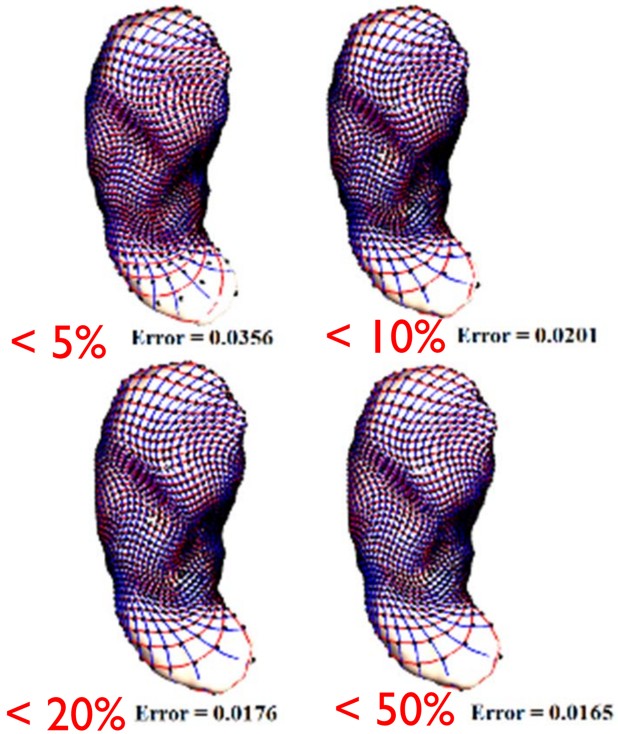

Bijectivity preservation

Demonstration:

Fourier decomposition of coordinate functions:

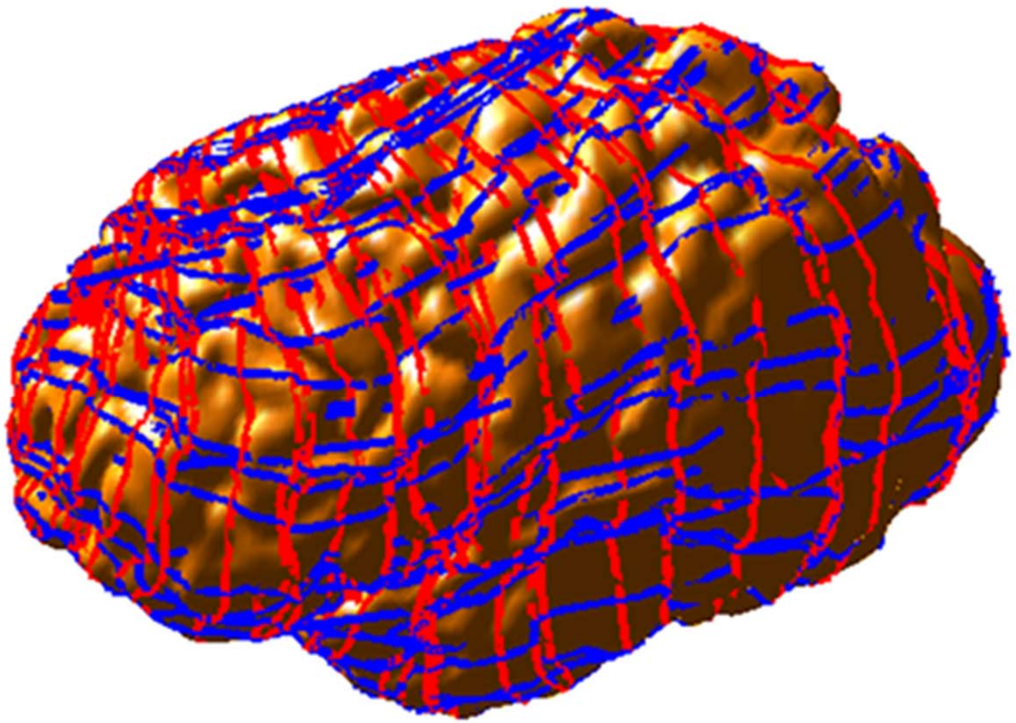

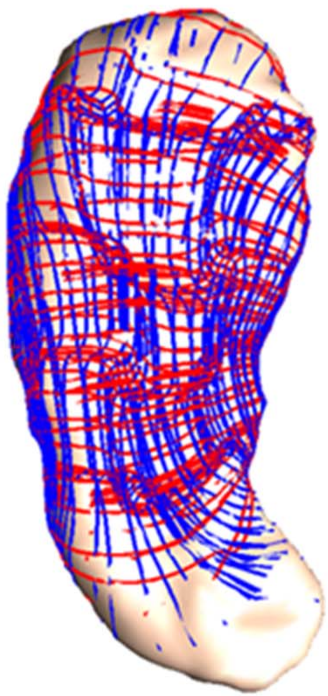

Outline:

- Motivation
- Beltrami coefficient & bijective deformation
- Proposed methods
  - Extraction of bijective deformation
  - Multiscale decomposition of deformations
- Experimental results

Extraction of deformation

- Formulate a foldover-free deformation as a bijective transformation of the domain in which the shape is embedded.
- An object is often captured by an image.
- Suppose the image of the object at the initial (t=0) and final (t=1) times are respectively:

$$I_1 : D \to \mathbb{R} \quad \text{and} \quad I_2 : D \to \mathbb{R}$$

- Extract the deformation by finding the image registration:

$$f : D \to D$$

where: $f \in W^{2,2}$

Image registration model using Beltrami coefficient

Large deformation image registration models:

Solve the optimization problem over the space of Beltrami differentials:

$$f = \mathbf{argmin}_{g:S_1 \to S_2} E_{LM}(\mu(g)) := \mathbf{argmin}_{g:S_1 \to S_2} \left\{ \int_{S_1} |\nabla \mu(g)|^2 + \alpha \int_{S_1} |\mu(g)|^p \right\}$$

subject to:

- $\mathbf{C}$(i) $f(p_i) = q_i$ for $1 \leq i \leq m$; (Landmark constraints)
- $\mathbf{C}$(ii) $||\mu(f)||_\infty < 1$. (bijectivity)

(Landmark-based registration algorithm)

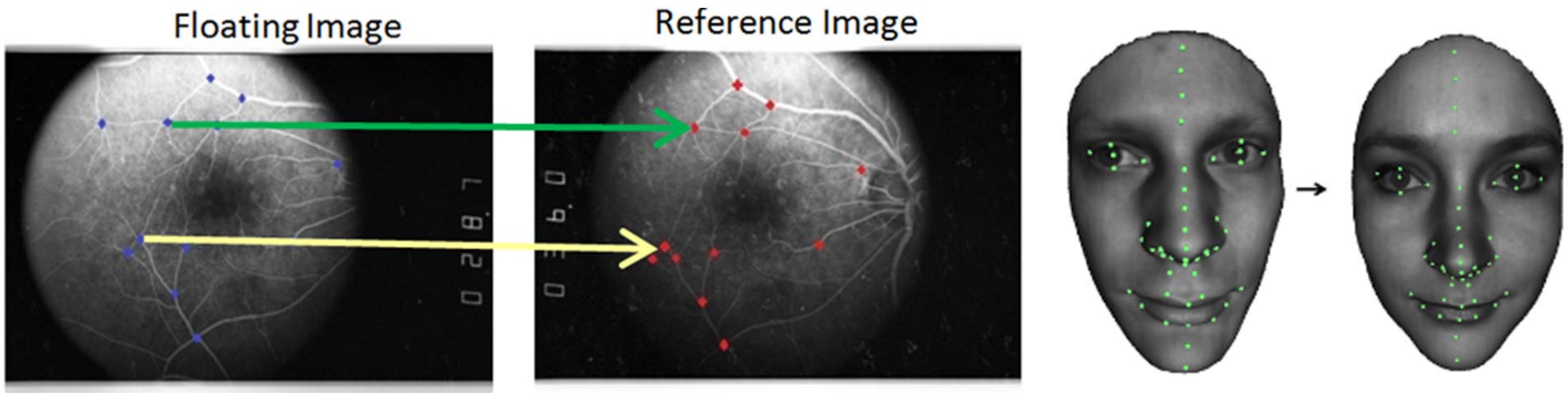

Landmark correspondences are given to guide the registration

Image registration model using Beltrami coefficient

Hybrid image registration models:
(Combining landmark correspondences and intensity matching)

Solve the optimization problem over the space of Beltrami differentials:

$$f := \mathbf{argmin}_{g:S_1 \to S_2} \left\{ \int_{S_1} |\nabla \mu(g)|^2 + \alpha \int_{S_1} |\mu(g)|^p + \beta \int_{S_1} (I_1 - I_2(g))^2 \right\}$$

Intensity matching term

subject to:

- $\mathbf{C}$(i) $f(p_i) = q_i$ for $1 \leq i \leq m$; (Landmark constraints)
- $\mathbf{C}$(ii) $||\mu(f)||_\infty < 1$. (bijectivity)

(Hybrid registration algorithm)

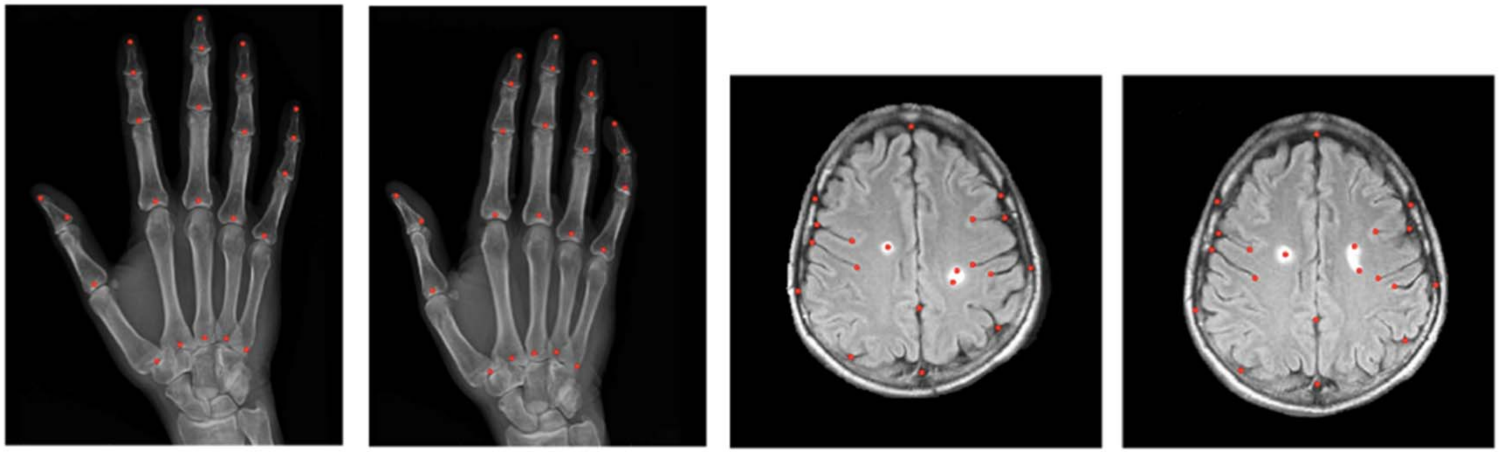

Finding image registration that matches landmarks and intensities

QC Registration model for large deformation

Splitting method to solve the optimization problem:

Strategy :

Transform the problem :

$$(\nu^*, f^*) = \mathbf{argmin}_{(\nu,f)} \alpha \int |\nu|^2 + \beta \int |\nabla \nu|^2 + \gamma_n \int |\nu - \mu(f)|^2$$

subject to :

- $\|\nu\|_\infty < 1$;
- $f(p_i) = q_i \rightarrow$ (Landmark constraints).

Idea :

$\Rightarrow$ Introduce auxiliary variable f

$\Rightarrow$ Alternate optimization over f and ν to decouple the minimization

QC Registration model for large deformation

Splitting method to solve the optimization problem:

$$\mathbf{argmin}_{\nu,f} \int \alpha|\nu|^2 + \beta|\nabla\nu|^2 + +\gamma \int |\nu - \mu(f)|^2$$

$$\Downarrow$$

A

Minimize (fixing f_n):

$$\mu_{n+1} = \mathbf{argmin}_{\nu} \int \alpha|\nu|^2 + \beta|\nabla\nu|^2 + \int |\nu - \mu(f_n)|^2 \tag{9}$$

B

Minimize (fixing μ_{n+1}):

$$f_{n+1} = \mathbf{argmin}_{f} \int |\mu_{n+1} - \mu(f)|^2 \tag{10}$$

Alternatively update μ_n and f_n using (A) and (B).

Registration model for large deformation

Experimental results:

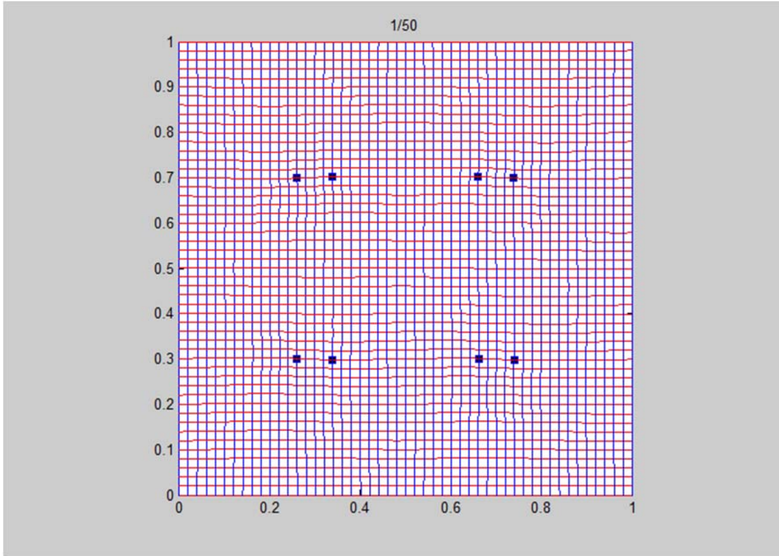

Large deformation landmark registration

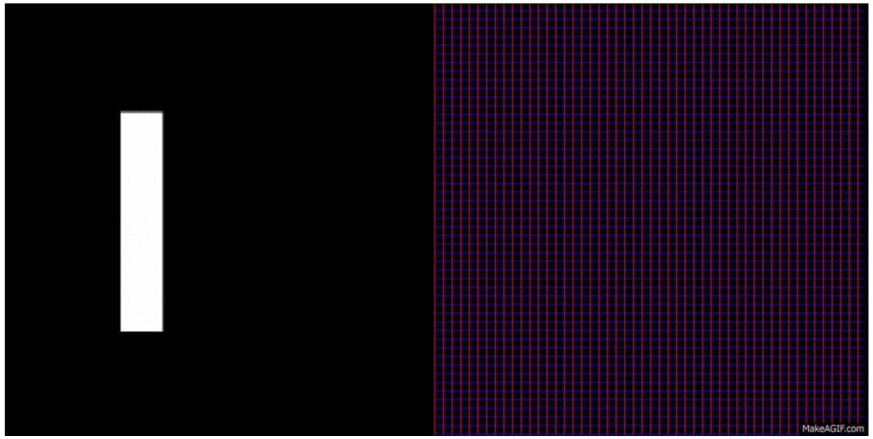

Large deformation hybrid registration

Registration model for large deformation

Experimental results:

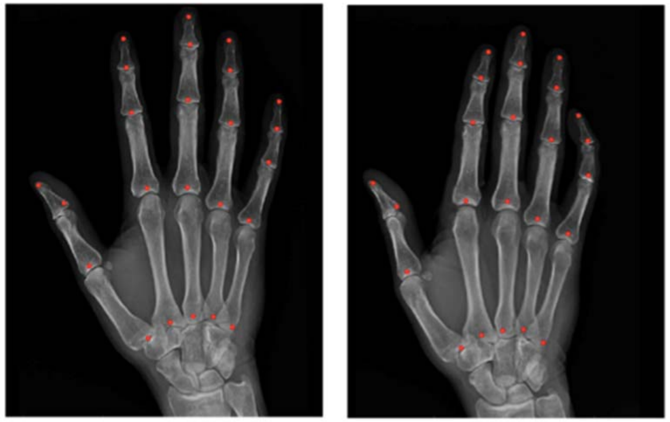

(a) Image 1(Hand) (b) Image 2(Hand)

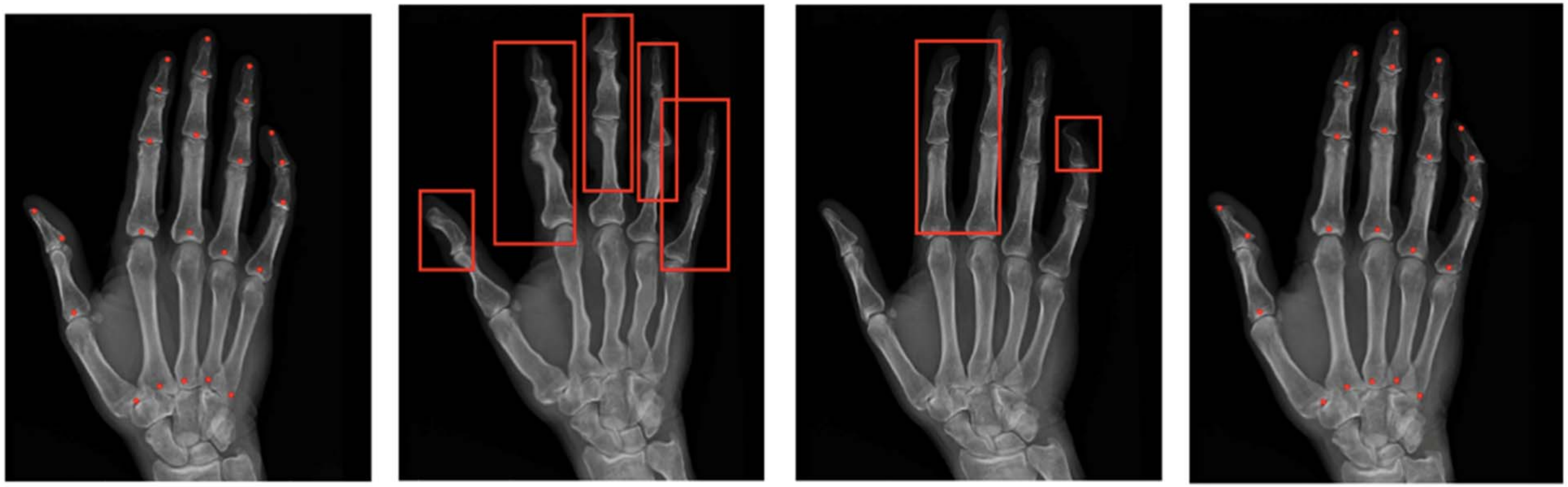

(a) Image 2 (Target) (b) Deformed image (Landmark) (c) Deformed image (Intensity) (d) Deformed image (Hybrid)

Applications of QC Registration

Medical applications:

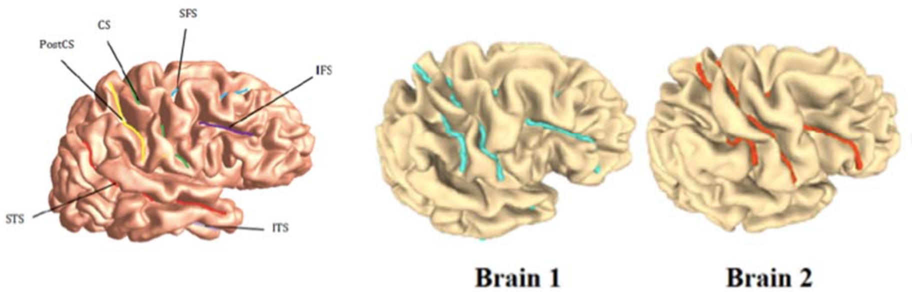

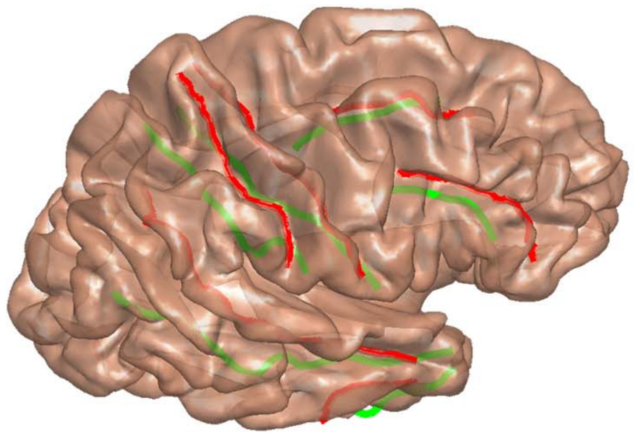

Brain surface registration (find one-one correspondence) for brain cortical surface comparison

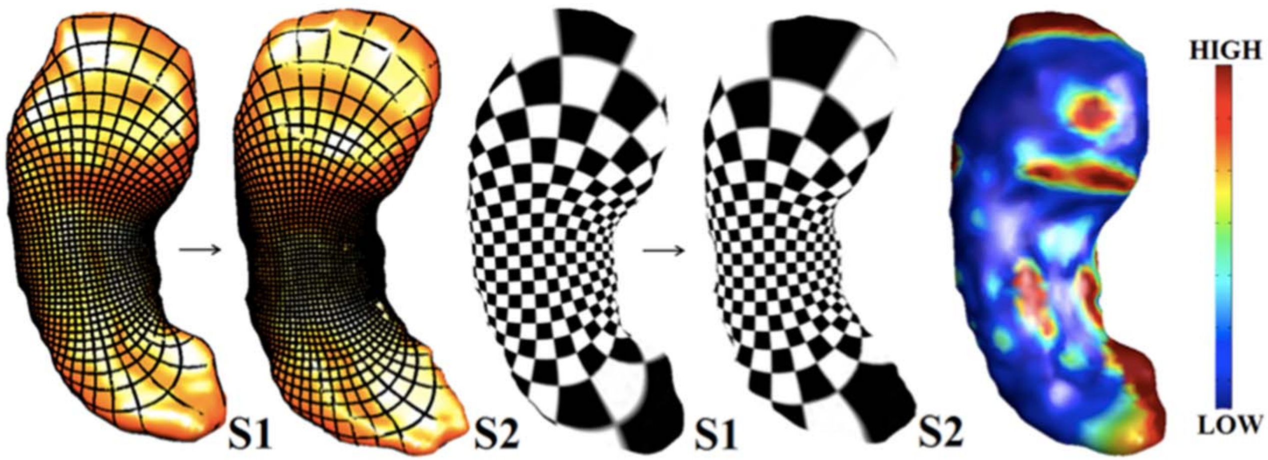

$$E_{shape}(\mu) = \alpha\int_D |\mu|^2 + \beta\int_D (H_1 - H_2(f^\mu))^2 + \gamma\int_D (K_1 - K_2(f^\mu))^2$$

Geometric matching Hippocampus registration to analyze Alzheimer's disease

Outline:

- Motivation
- Beltrami coefficient & bijective deformation
- Proposed methods
  - Extraction of bijective deformation
  - Multiscale decomposition of deformations
- Experimental results

Multiscale decomposition of deformations

Key idea:

- *Extract bijective deformation $f : D \to D$ using image registration;*
- *Represent the bijective transformation using Beltrami coefficient:*

$$\mu(f)(z) = \left(\frac{\partial f}{\partial \bar{z}}\right) \Big/ \left(\frac{\partial f}{\partial z}\right)$$

- *Wavelet transform on the Beltrami coefficient to obtain a multi-scale decomposition of the Beltrami coefficient.*
- *Obtain the multiscale components of the deformation by reconstructing the transformation from BCs, through solving:*

$$\nabla \cdot (A \nabla u) = 0 \text{ and } \nabla \cdot (A \nabla v) = 0, \quad \text{where } A = \begin{pmatrix} \alpha & \beta \\ \beta & \gamma \end{pmatrix}$$

Subject to suitable boundary conditions.

Determined by BC

Multiscale representation (MSR) of deformations

- *Let* $\Phi(x,y)$ *,* $\Psi^{(1)}(x,y)$ *,* $\Psi^{(2)}(x,y)$ *and* $\Psi^{(3)}(x,y)$ *be the 2D scaling and wavelet functions. Define:*

$$\Phi_{j,k_1,k_2}(x,y) := 2^j \Phi(2^j x - k_1, 2^j y - k_2)$$
$$\Psi^{(i)}_{j,k_1,k_2}(x,y) := 2^j \Psi^{(i)}(2^j x - k_1, 2^j y - k_2)$$

- *Given a bijective transformation* f *representing a foldover-free deformation. Let* $\mu(f)$ *be the BC of* f *.*
- *Decompose the BC as follows:*

$$\mu(f)(x,y) = \sum_{i=1}^{3} \sum_{l\in\mathbb{Z}} \sum_{k_1\in\mathbb{Z}} \sum_{k_2\in\mathbb{Z}} \hat{\mu}(i,l,k_1,k_2)\Psi^{(i)}_{l,k_1,k_2}(x,y)$$

where: $\hat{\mu}(i,l,k_1,k_2) = \langle \mu(f), \Psi^{(i)}_{l,k_1,k_2} \rangle$

Multiscale representation (MSR) of deformations

Some terminologies:

The collection of coefficients $\{\hat{\mu}(i,l,k_1,k_2)\}_{1\leq i\leq 3, j, k_1, k_2\in\mathbb{Z}}$ are called the (wavelet) decomposition coefficients of the deformation f.

Let $U_j := \mathcal{T}(\mathbf{Span}(\{\Phi_{j,k_1,k_2}\}_{k_1,k_2\in\mathbb{Z}}))$, where $\mathcal{T}$ is the truncation operator to enforce the supreme norm of a complex-valued function to be strictly less than 1. U_j is called the set of deformation distortions at scale j.

Define: $V_j := \mathbf{LBS}(U_j)$, where $\mathbf{LBS}$ converts a Beltrami coefficient to its associated quasi-conformal map. V_j is called the set of deformations at scale j.

Let

$$\mathcal{P}_J(\mu(f)) := \mathcal{T}\left(\sum_{i=1}^{3}\sum_{j<J}\sum_{k_1,k_2\in\mathbb{Z}} \hat{\mu}(i,j,k_1,k_2)\Psi^{(i)}_{j,k_1,k_2}(x,y)\right).$$

$\mathcal{P}_J$ is called the projection of $\mu(f)$ to the distortion component at scale J. $\mathcal{P}_J(\mu(f))$ is called the distortion component at scale J.

Multiscale representation (MSR) of deformations

Definition of MSR of a foldover-free deformation

Let $f_j := \mathbf{LBS}(\mathcal{P}_j(\mu(f))) : \mathbb{C} \to \mathbb{C}$. $f_j \in V_j$ is called the deformation component at scale j. The sequence $\{f_j : \mathbb{C} \to \mathbb{C}\}_{j \in \mathbb{Z}}$ is called the multi-scale representation (**MSR**) of the deformation f.

Some remarks:

- *The truncation operator can simply be chosen as:*

$$\mathcal{T}(\mu) = \mathbf{T}(|\mu|)\frac{\mu}{|\mu|}$$

where $\mathbf{T} : [0, +\infty) \to [0, 1)$ is a monotonically increasing function such that $\mathbf{T}(x) = x$ for $x \in [0, 1-\epsilon]$ and $\lim_{x \to +\infty} \mathbf{T}(x) = 1$.

Some theoretical results (I):

Theorem: $\bigcap_{j\in\mathbb{Z}} V_j = \{\mathbf{Id} : \mathbb{C} \to \mathbb{C}\}$, where $\mathbf{Id}$ is the identity map of $\mathbb{C}$.

Remarks:

- *In fact:* $U_j \subseteq U_{j+1}$ and $V_j \subseteq V_{j+1}$ for all $j \in \mathbb{Z}$.
- *Also, our proposed method decomposes a deformation into its MSR:*

$$\{f_j \in V_j\}_{j\in\mathbb{Z}}$$

- *The above theorem shows that our proposed MSR* $\{f_j \in V_j\}_{j\in\mathbb{Z}}$ *starts from an identity transformation, which is called the trivial deformation.*
- *The sequence of deformation will capture finer and finer details.*

Some theoretical results (2):

Theorem: Given an accuracy $\epsilon > 0$, there exist a deformation f^J at certain scale J whose distortion resemble to the distortion of f up to the prescribed accuracy. In other words, for all $\epsilon > 0$, there is a $J \in \mathbb{Z}$ and a bijective transformation $f^J \in V_J$ such that $\|\mu(f^J) - \mu(f)\|_2 < \epsilon$. Also, $\lim_{j\to\infty} \|\mu(f) - \mathcal{P}_j(\mu(f))\|_2 = 0$.

Remarks:

- Our algorithm allows us to project an input deformation to a component, such that its deviation from the original deformation with respect to the local geometric distortion is within a prescribed error.

Some theoretical results (3):

Theorem: Suppose $f : \mathbb{C} \to \mathbb{C}$ is a quasi-conformal map. Suppose $\mathcal{P}_j$ is the projection operator of the Beltrami coefficient $\mu(f)$ of f to the distortion component at scale j. Let f_j be the deformation component at scale j. Then, f_j converges locally uniformly to the original deformation f.

Remarks:

- *The above theorem shows that the deformation component converges to the original deformation as j increases.*
- *In other words, our decomposition gives a sequence of transformations, which capture finer and finer geometric details from the coarsest level, until it resembles to the original deformation.*

Some theoretical results (4):

Theorem: Suppose $\mu : \Omega \to \mathbb{C}$, where Ω is some bounded open set, satisfies $\|\mu\|_\infty < 1$, then the associated mapping $f^\mu : \Omega \to \mathbb{C}$ is locally homeomorphic (that is, folding-free). Furthermore, if Ω and Ω_2 (the image of f^μ) are both simply-connected, then $f^\mu : \Omega \to \mathbb{C}$ is globally bijective.

Remarks:

- The above theorem tells us the bijectivity of the extracted deformation components can be achieved by enforcing the norm of BC to be strictly less than one.
- All deformation components from our multiscale decomposition are foldover free.

Some theoretical results (5):

Theorem: Let f be a deformation on $\Omega \subset B_R := \{\mathbf{x} : |\mathbf{x} \leq R\}$. Assume that f is extended to ∂B_R with $f|_{B_R} = \mathbf{Id}$. Suppose f is composed of various deformation components $\{f_j\}_{j\in J}$ of different scales, whose **BC**s are given by $\{\mu_j\}_{j\in J}$. Let $\widetilde{f}$ be another deformation on Ω and denotes its associated **BC** as $\widetilde{\mu}$. For each $j \in J$, if $|\mu_j|, |\widetilde{\mu}| \leq k\mathcal{X}_\Omega$ for some $0 \leq k < 1$ and $\|\tilde{\mu} - \mu_j\|_{L^{pt/(t-1)}(B_R)} < \epsilon$ for $2 \leq p < 2t < 1 + 1/k$, then

$$\left\|\widetilde{f} - f_j\right\|_{L^p(\Omega)} < C_1(k,t,R)\epsilon \quad \text{and} \quad \left\|\nabla\widetilde{f} - \nabla f_j\right\|_{L^p(\Omega)} < C_2(k,t,R)\epsilon.$$

for some positive constants $C_1(k,t,R)$ and $C_2(k,t,R)$.

Remarks:

- *The above theorem show that the extracted deformation component and its first derivatives are close to the actual ones in Lp-sense, when the extracted BC is close to the BC of the actual deformation component.*
- *The application of BC in our algorithm can lead to good approximations of the deformation components up to their first derivatives.*

Some theoretical results (6):

Theorem: Let f be a deformation on $\Omega \subset B_R$. Assume that f is extended to ∂B_R with $f|_{B_R} = \mathbf{Id}$, whose **BC** is given by μ. If μ is measurable, then $f \in W^{1,2}$. And suppose $\mu \in W^{1,p}$, we have:

- $f \in W^{2,p}_{loc}(\mathbb{C})$ if $p > 2$;
- $f \in W^{2,q}_{loc}(\mathbb{C})$ for every $q < 2$ if $p = 2$;
- $f \in W^{2,q}_{loc}(\mathbb{C})$ for every $q < q_0$, where $\frac{1}{q_0} = \frac{1}{p} + \frac{k}{k+1}$, if $1 + k < p < 2$.

Remarks:

- *The above theorem shows that the differentiability of the extracted transformation is one degree higher than its associated BC.*
- *The application of BC in our algorithm enhances the differentiability (smoothness) of the extracted deformation component.*

Algorithm:

Algorithm 1 *Multi-scale decomposition of a deformation*

1: Compute the registration f between I_1 and I_2.
2: Compute the Beltrami coefficient $\mu(f)$ of f.
3: Compute the wavelet expansion of $\mu(f)$ to obtain $\hat{\mu}(i, j, k_1, k_2)$ for $1 \leq i \leq 3$, $j, k_1, k_2 \in \mathbb{Z}$.
4: For each $j \in \mathbb{Z}$, compute $\mathcal{P}_j(\mu(f))$ and $f_j := \mathbf{LBS}(\mathcal{P}_j(\mu(f)))$.
5: For each $j \in \mathbb{Z}$, compute $I^{(j)} := I_1 \circ f_j^{-1}$.

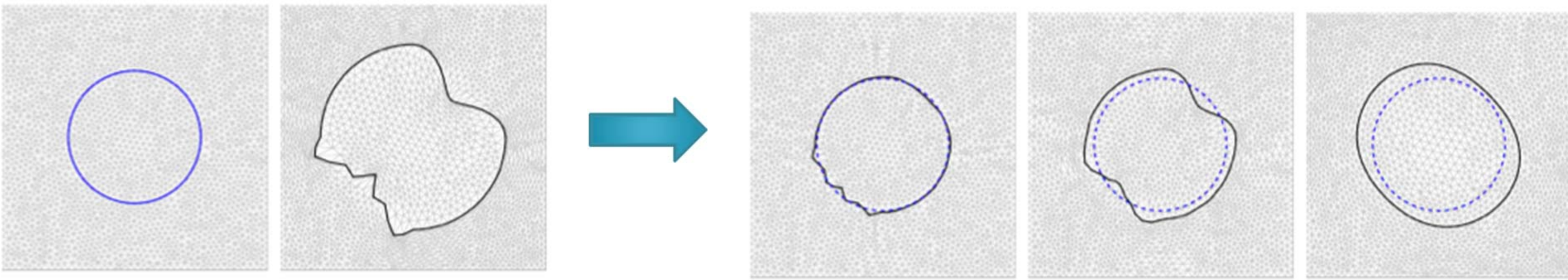

(a) Original (b) Registered (c) Local (d) Intermediate (e) Global

Outline:

- Motivation
- Beltrami coefficient & bijective deformation
- Proposed methods
  - Extraction of bijective deformation
  - Multiscale decomposition of deformations
- Experimental results

Experimental results

Example 1:

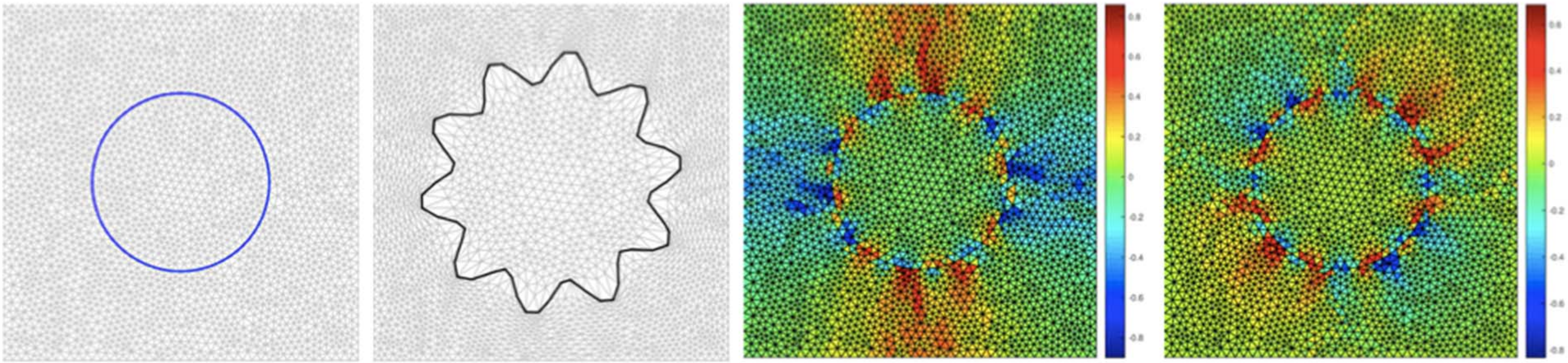

(a) Original mesh (b) Deformed mesh (c) Re(μ) (d) Imag(μ)

Deformation from a circle to a star-shaped contour. The unit circle and the deformed star-shaped contour are shown in (a) and (b) respectively. The boundaries of the object in the original and deformed images are labeled in blue and black respectively as landmarks. (c) and (d) show the real and imaginary part of the BC associated to the deformation.

Experimental results

Example 1: (Continued)

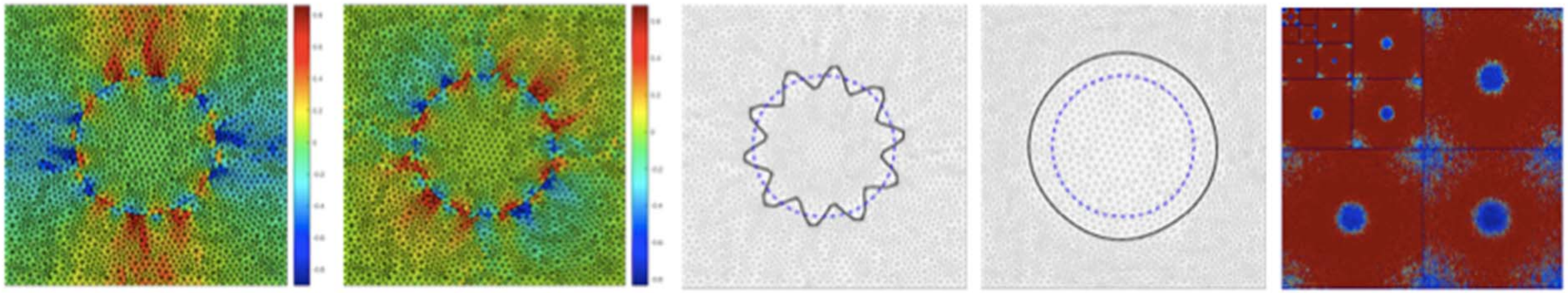

(a) Re(μ) (b) Imag(μ) (c) Local (d) Global (e) Spectrum

Multi-scale representation of the deformation from a circle to a star-shaped contour. (a) and (b) respectively show the reconstruction of the real and imaginary part of BC using the full set of coefficients. (c) and (d) show the local and global deformation components respectively. (e) shows the spectrum of the wavelet decomposition coefficients.

Experimental results

Example 2:

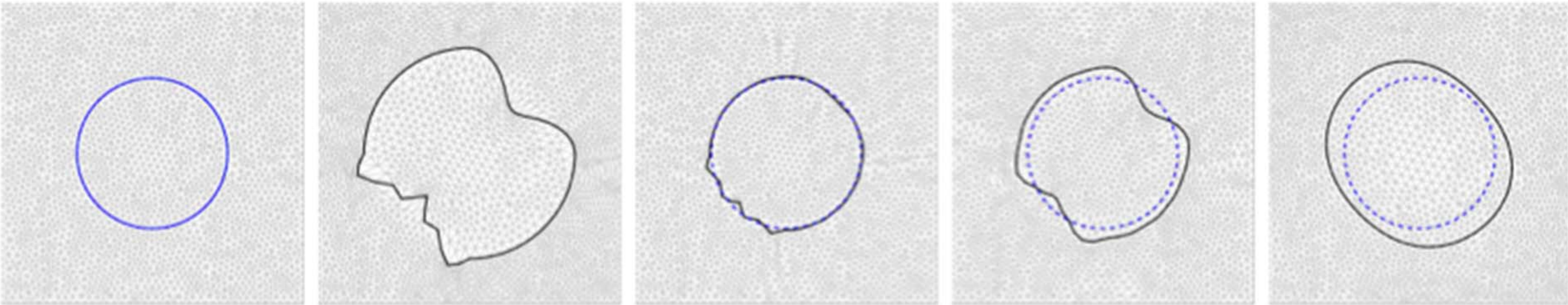

(a) Original (b) Registered (c) Local (d) Intermediate (e) Global

(a) and (b) show the original mesh and the registration result of Example 2, where the landmarks and targets are marked in blue and black respectively. (c), (d) and (e) show the local, intermediate and global deformation components respectively.

Experimental results

Example 3:

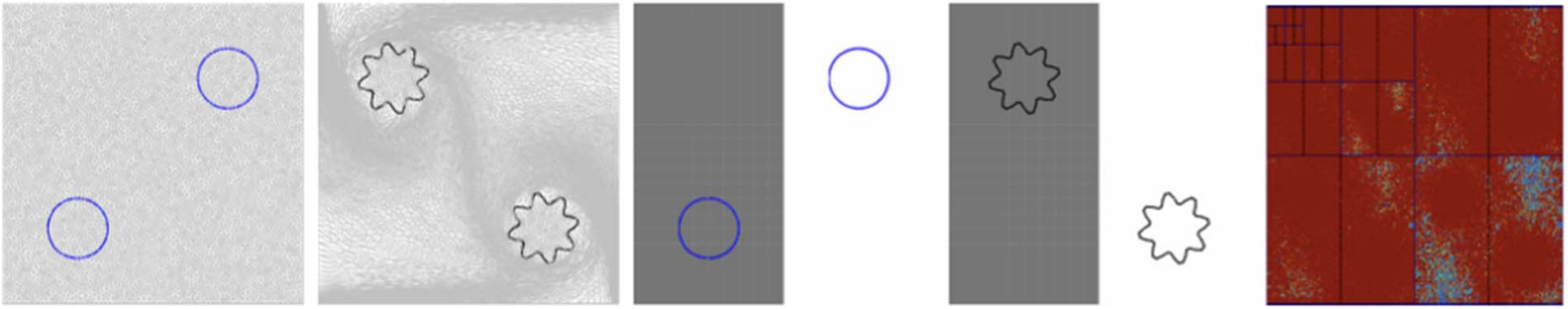

(a) Original (b) Registered (c) Mask on (a) (d) Mask on (b) (e) Spectrum

(a) and (b) show the original mesh and the registration result of Example 3, where the landmarks and targets are marked in blue and black respectively. (c) and (d) show the mask for the wavelet decomposition coefficients for extracting the regional local and global deformation components. (e) shows the spectrum of the wavelet decomposition coefficients. The black dotted vertical line shows the boundary of the mask introduced.

Experimental results

Example 3: (Continued)

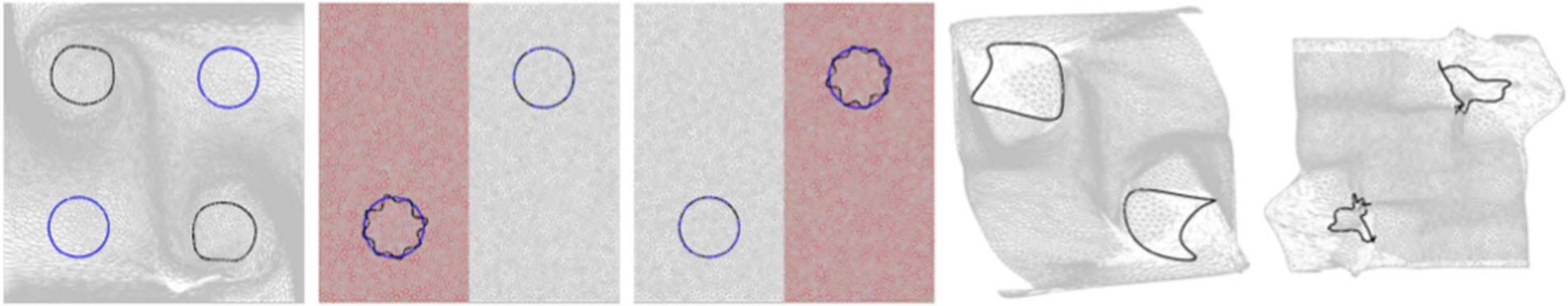

(a) Global (b) First local (c) Second local (d) Global (e) Local

(a), (b) and (c) show the global, left and right local deformation components extracted by our proposed algorithm. (d) and (e) show the extraction results obtained by directly applying the wavelet transform on the vector fields of the mapping. Note that abnormal squeezing and foldovers can be observed.

Experimental results

Example 4:

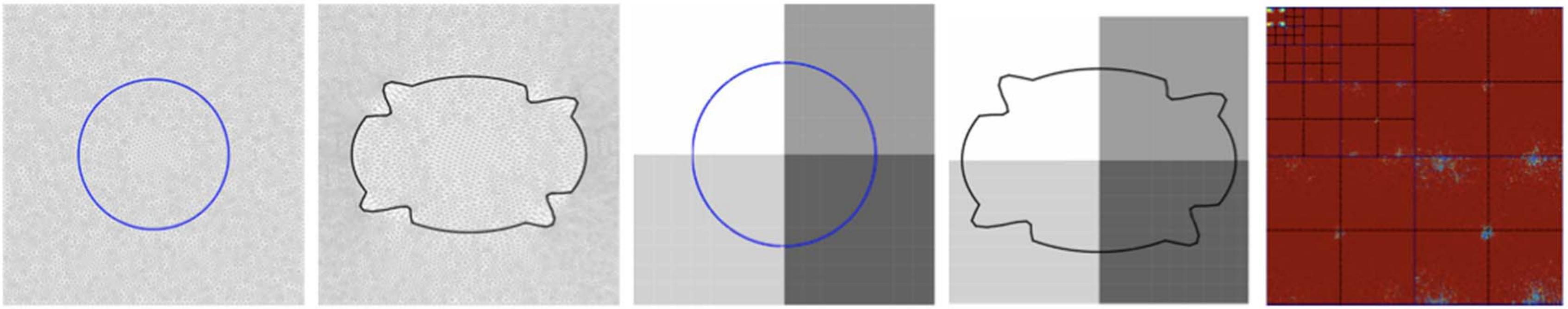

(a) Original (b) Deformed (c) Mask on (a) (d) Mask on (b) (e) Spectrum

(a) and (b) show the original and deformed mesh of Example 4. (c) and (d) shows the mask for extracting the decomposition coefficients of Example 4, which are divided into four regions. (e) shows the spectrum of the wavelet decomposition coefficients of Example 4.

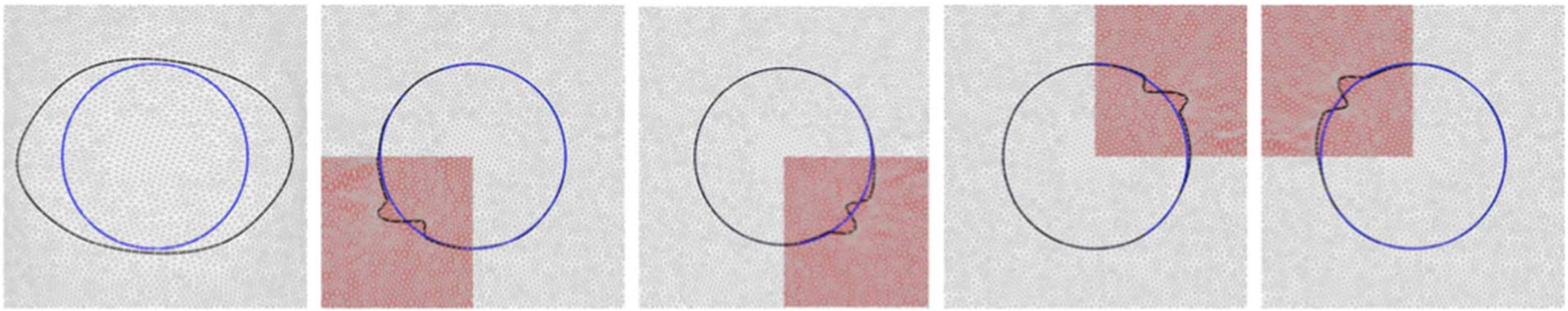

(a) Global (b) First local (c) Second local (d) Third local (e) Fourth local

(a) shows the extracted global deformation component of Example 4. (b), (c), (d) and (e) shows the local deformation components at the bottom-left, bottom-right, top-right and top-left regions respectively.

Experimental results

Example 5: Spine deformation

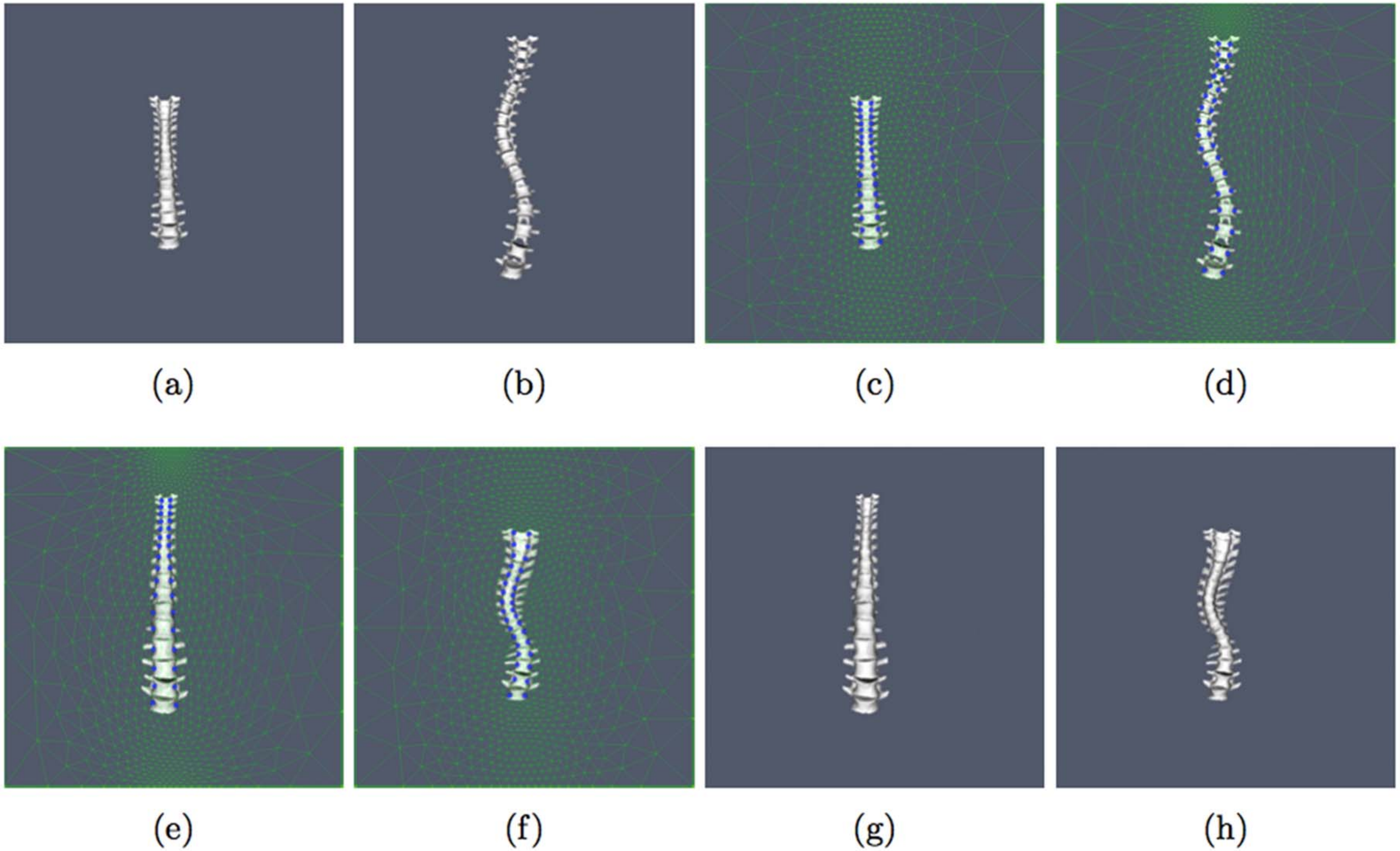

(a) shows the original spine image. (b) shows the deformed spine image of a grown-up patient. (c) and (d) respectively show the landmark points in (a) and (b) marked in blue. A triangular mesh is built on each images. (e) and (f) show the global and local components of the spine deformation extracted by our proposed algorithm. (g) and (h) show the corresponding deformed images.

Experimental results

Example 6: Corpus Callosum

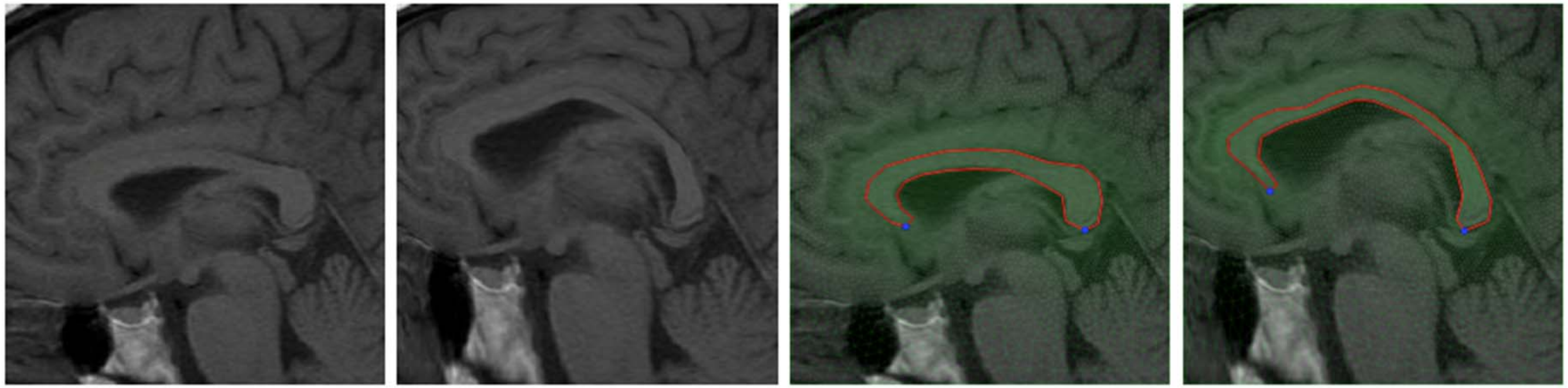

(a) (b) (c) (d)

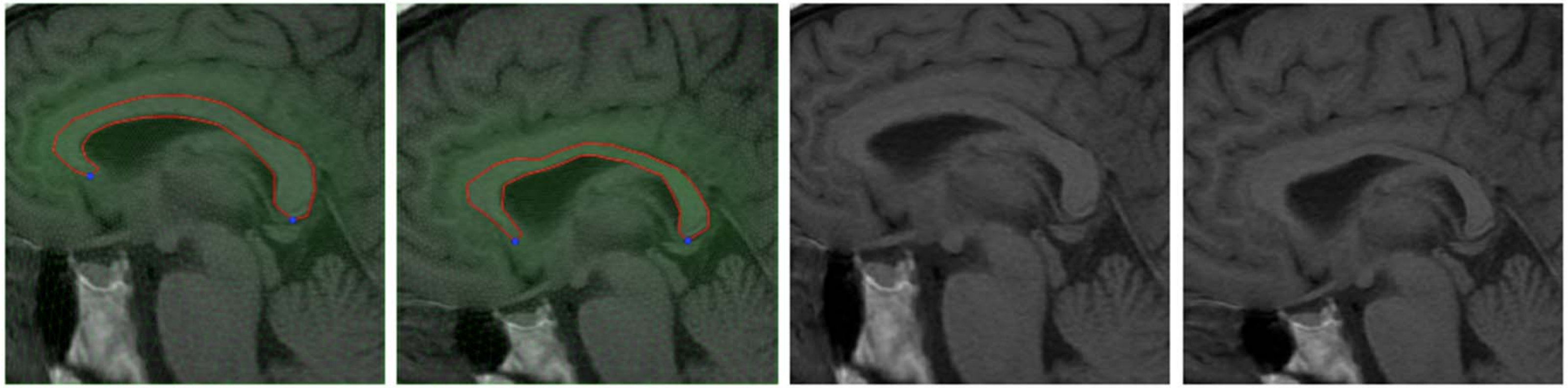

(e) (f) (g) (h)

(a) shows the image of a healthy corpus callosum. (b) shows the image of the corpus callosum of a patient suffering from progressive supranuclear palsy (PSP). (c) and (d) show the feature landmarks (blue and red) which extract the corpus callosum in (a) and (b) respectively. Triangular meshes are built on each images for registration. (e) and (f) show how the mesh of the image from the healthy subject is deformed under the extracted global and local deformations respectively. The deformed images by the global and local deformations are shown in (g) and (h) respectively.

Experimental results

Example 7: Corpus Callosum

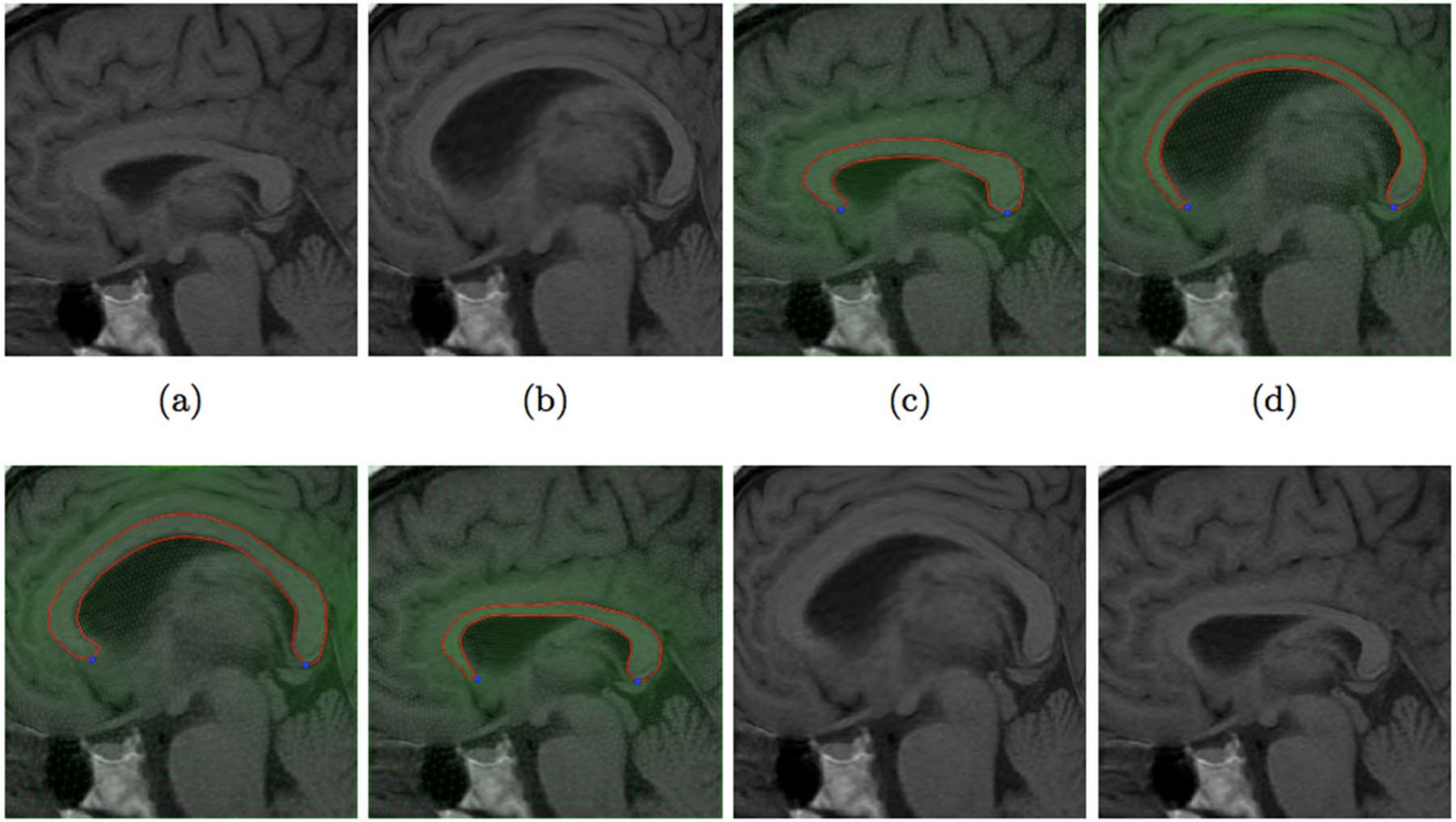

(a) (b) (c) (d) (e) (f) (g) (h)

(a) shows the image of a healthy corpus callosum. (b) shows the image of the corpus callosum of a patient suffering from Normal pressure Hydrocephalus (NPH). (c) and (d) show the feature landmarks (blue and red) which extract the corpus callosum in (a) and (b) respectively. Triangular meshes are built on each images for registration. (e) and (f) show how the meshes of the image from the healthy subject is deformed under the extracted global and local deformations respectively. The deformed images by the global and local deformations are shown in (g) and (h) respectively.

Conclusion:

- Described a method for the multiscale decomposition of deformation using Beltrami coefficients;
- Using BC, we can effective preserve the bijectivity of the bijective deformation (modeled as a bijective transformation)
- A deformation can be decomposed into different components with various geometric scales and locations.

Future works:

- Applications to cardiac motion analysis;
- Extension to n-D cases;
- Restoration of turbulence-distorted video with moving objects.

Comparison with (x-y) based methods

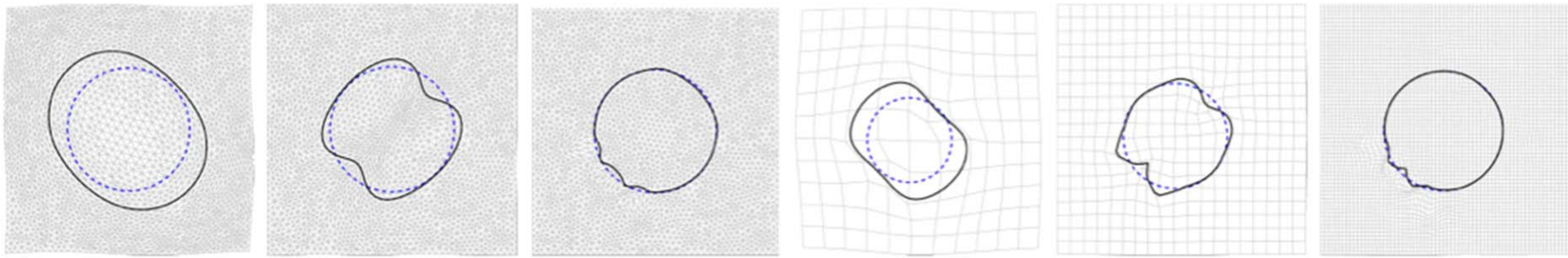

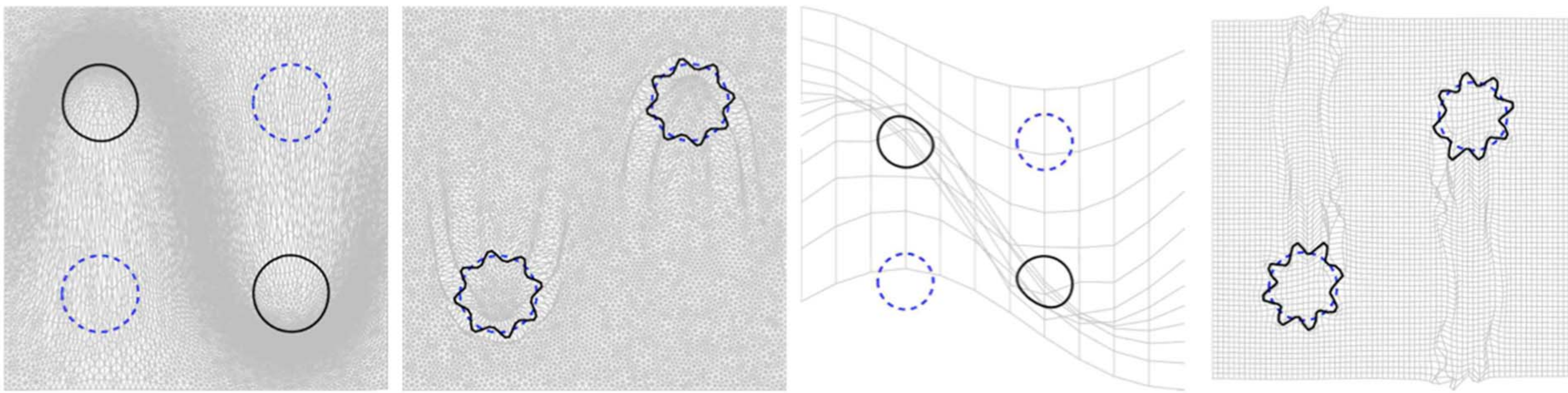

Comparison with (x-y) based methods